Evaluating parameterisations of subgrid-scale variability

Johannes Quaas[1], Verena Grützun[2], Vera Schemann[2] and Torsten Weber[3]

(1) Universität Leipzig, Insitute for Meteorology, Stephanstr. 3, 04103 Leipzig, johannes.quaas@uni-leipzig.de
(2) Max Planck Institute for Meteorology, Bundesstr. 53, 20146 Hamburg
(3) Helmholtz-Zentrum Geesthacht, Climate Service Center, Fischertwiete 1, 20095 Hamburg

ABSTRACT

Parameterisations of fractional cloudiness in large-scale atmospheric models rely on information about the subgrid-scale variablity of the total water specific humidity, q_t, provided in form of a probability density function (PDF). In this contribution, four different approaches to evaluate such total-water PDFs are discussed: (i) Satellite spectroradiometers with high spatial resolution allow to construct at the scale of model grid boxes a histogram, and subsequently to derive the moments of the PDF, of the vertical integral of q_t. This can be compared to the same quantity diagnosed from the model parameterisation. Although the vertical integral mostly focuses on the boundary layer, and involves issues in grid-boxes with orographic variability, it allowed nevertheless in the example presented to pinpoint deficiencies of a model parameterisation. (ii) Assuming a simple PDF shape and saturation within clouds, the simple "critical relative humidity" metric can be derived from infrared sounders and/or cloud lidar in combination with reanalysis data with a vertical resolution. It allows to evaluate the underlying PDF of any cloud scheme, but is sensitive to the assumptions. (iii) Supersites with a combination of ground-based lidar, radar and microwave data provide high-resolution high-quality reference data. In a "virtual reality" framework, we showed, however, that it is difficult to evaluate higher moments of a spatial PDF with this temporally-varying data. (iv) From a hierarchy of models from general circulation models to direct numerical simulations, we find that the variance of the q_t follows a power-law scaling with an exponent of about -2. This information is very useful to improve the parameterisations.

1 Introduction

Current large-scale numerical models of the atmosphere diagnose or predict a fractional cloud cover to compute the effect of cloudiness on radiation. For example, Sundqvist et al. (1989) allow for fractional cloudiness for grid-box mean relative humidities, r, above a "critical relative humidity", r_c, below 100%. Tompkins (2002) predicts variance and skewness of a beta-function PDF, with mainly detrainment from deep convection as a source of skewness, turbulence as a sink of variance and precipitation formation as a sink for skewness. In the implementation in the ECHAM5 general circulation model (GCM), only symmetric or positively skewed PDFs are allowed (Roeckner et al., 2003). It is also possible to use cloud water and cloud cover as prognostic variables, in which case the assumptions about the PDF of q_t are not explicit in the model (Tiedtke, 1993).

A thorough evaluation of the subgrid-scale PDF of q_t requires accurate observations of water vapour and cloud liquid- and ice water at high temporal and spatial resolution for various layers in the troposphere at a large - ideally global - scale. Such data is not available. In this contribution, we propose several pathways to exploit the existing data for an evaluation of PDFs of q_t as the basis of GCM cloud parameterisations.

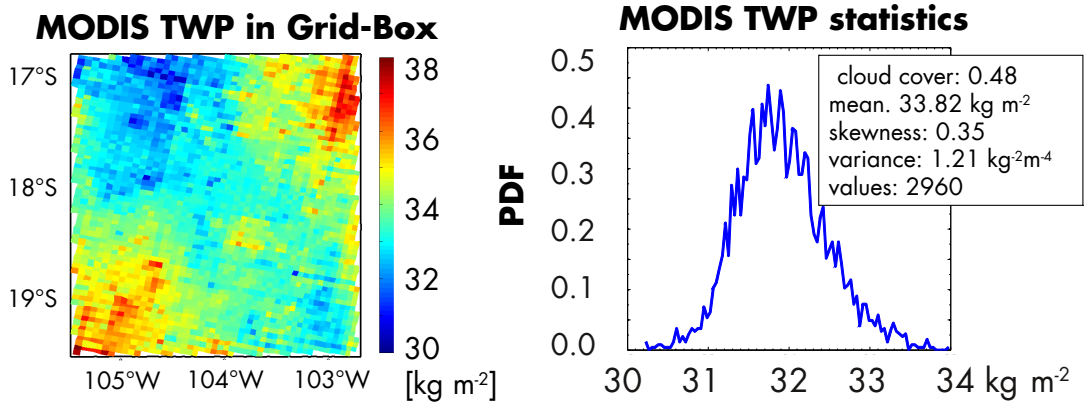

Figure 1: Example of a distribution of MODIS-derived total water path [kg m^{-2}] within one GCM gridbox of approx. T42 size (a), and corresponding histogram with moments of the PDF (b).

2 Evaluation of the total water path PDF

The MODerate Resolution Imaging Spectroradiometer (MODIS) retrieves at a horizontal resolution of 5x5 km^2 precipitable water, or the vertical integral of specific humidity, cloud liquid water path and cloud ice water path (Platnick et al., 2003). In order to evaluate the horizontal variability at a scale of about 310x310 km^2 (corresponding to the typical T42 spectral resolution of, e.g., the ECHAM5 GCM), up to about 3800 MODIS retrievals are available to construct a histogram. Precipitable water is retrieved only in clear sky situations yet dominates the total water path (TWP). Our approach is to use in cloudy situations the up to nine nearest clear-sky satellite pixels to interpolate a value of precipitable water in the cloudy pixel. The TWP in this pixel is then the sum of the so-derived precipitable water and the liquid- and ice water paths. Only MODIS retrievals with a high quality assurance flag are considered. Then at each grid-point globally and for each satellite overpass, from the MODIS-derived histograms variance and skewness of the TWP are computed (Fig. 1; Weber et al., 2011). The variance, shown in Fig. 2 as the geographical distribution in absolute terms, is largest in the low latitudes where the TWP is largest. More homogeneous distributions are found in general over the oceans than over land. Note that TWP and its distribution are dominated by the atmospheric boundary layer due to the typically exponential decrease in specific humidity with height. The derived skewness shows even in the annual mean a much noisier distribution. There are some emerging features, though, such as the frequently negative skewness in the low latitudes, and the general tendency for more positive skewness over land than over ocean. Using the parameterised subgrid-scale PDF of q_t in the model (Tompkins, 2002), and applying a subcolumn sampler to compute the vertical integral using maximum-random overlap for clouds and maximum overlap for water vapour distributions (Räisänen et al., 2004), we diagnosed histograms

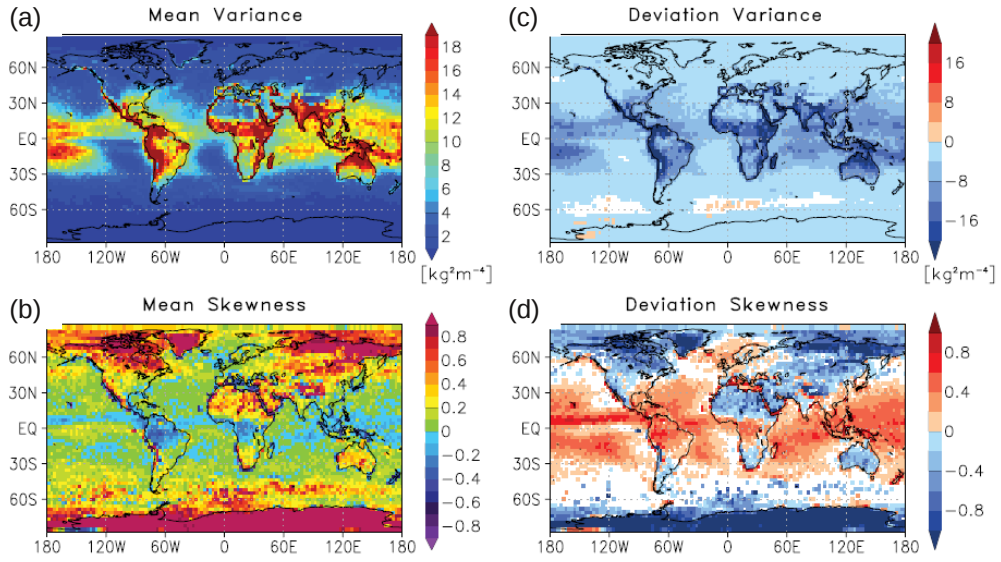

Figure 2: Annual-mean distribution for the MODIS-derived (a) variance and (b) skewness of TWP at a T42 resolution, and difference between the results of ECHAM5 with the Tompkins (2002) scheme and MODIS for (c) variance and (d) skewness.

of TWP, and subsequently the moments of its PDF, from ECHAM5 consistently with the satellite data (Weber et al., 2011). Fig. 2 shows the geographical distribution of the difference between the model results and the satellite results for the annual mean. The simulated variance is underestimated virtually everywhere, and particularly in the low latitudes where the observations-derived variance is large. Some issues with the method can also be seen. In grid-boxes with large orographic variability (e.g., the Andes and Himalaya mountains), there is a large TWP variability due to the differences in the depth of the atmospheric column. Since the model applies a smoothed orography, much less variance is simulated in these cases in the model. The model substantially overestimates skewness in the low latitudes, and over extratropical oceans. One reason for this is certainly that only positively skewed or symmetric distributions are possible, and allowing for negative skewness improves the comparison (Weber et al., 2011). Another reason for the particular bias in the tropics, and in this metric focusing on the boundary layer, is also that deep convection increases skewness due to detrainment in the upper and middle troposphere, but the dry convective downdrafts do not lead to negative skewness in the boundary layer next to convective towers in the current implementation of the Tompkins (2002) parameterisation. Over land, in turn, expecially in the extra-tropics, the simulated skewness is too low. Currently detrainment from deep convection is the only source for skewness, and other source processes in the extratropics are needed to match the observations.

3 Critical relative humidity as a metric for total water variance

The critical relative humidity is used as a parameter in the cloud scheme of Sundqvist et al. (1989), implemented in the ECHAM5 GCM by Lohmann and Roeckner (1996). Where the grid-box mean relative humidity, $\bar{r}$, exceeds this threshold, a cloud fraction, f, of

$$f = 1 - \sqrt{\frac{1-\bar{r}}{1-r_c}} \tag{1}$$

is diagnosed. It can be shown that a uniform PDF of q_t with a distribution width of $2\Delta q$ related to the saturation specific humidity, q_s, as a constant fraction, $\Delta q = \gamma q_s$, is equivalent to this formulation with $r_c = 1 - \gamma$. Thus, a low r_c corresponds to a large q_t subgrid-scale variability, and an r_c close to 1, to very homogeneous q_t distributions. The equation for the cloud fraction can be inverted to obtain r_c from cloud fraction and relative humidity,

$$r_c = 1 - \frac{1-\bar{r}}{(1-f)^2} \tag{2}$$

From this equation, r_c as a metric for the subgrid-scale variance of q_t can be inferred from the two large-scale quantities, f and $\bar{r}$. Data from the Atmospheric Infrared Sounder (AIRS; Susskind et al., 2003) provide such data. As an alternative, one can use cloud fraction from the Cloud-Aerosol Lidar and Infrared Pathfinder Satellite Observations (CALIPSO; Chepfer et al., 2010) in combination with relative humidity from the European Centre for Medium-Range Weather Forecasts Re-analysis (ERA-Interim; Simmons et al., 2006). Similarly, r_c can easily be diagnosed from any model output of cloud cover and relative humidity. The observations-derived r_c thus may serve to evaluate also cloud parameterisations different from the Sundqvist et al. (1989) one. Fig. 3 shows the profiles diagnosed from the two different observational datasets as well as from various climate model simulations (Quaas, 2012). This metric can be inferred globally and with vertical resolution. There are some caveats, though. Firstly, it is necessary to assume that within a cloud, the specific humidity is the saturation specific humidity. This assumption is fulfilled for liquid-water clouds, but not necessarily true for ice clouds. This might be a reason for the local maximum in the observations-based profiles (Fig. 3). Secondly, the underlying PDF is important. If one assumes a triangular rather than uniform PDF (Smith, 1990), r_c is computed from f and $\bar{r}$ as

$$r_c = 1 - \frac{3}{\sqrt{2}} \frac{1-\bar{r}}{(1-f)^{3/2}} \tag{3}$$

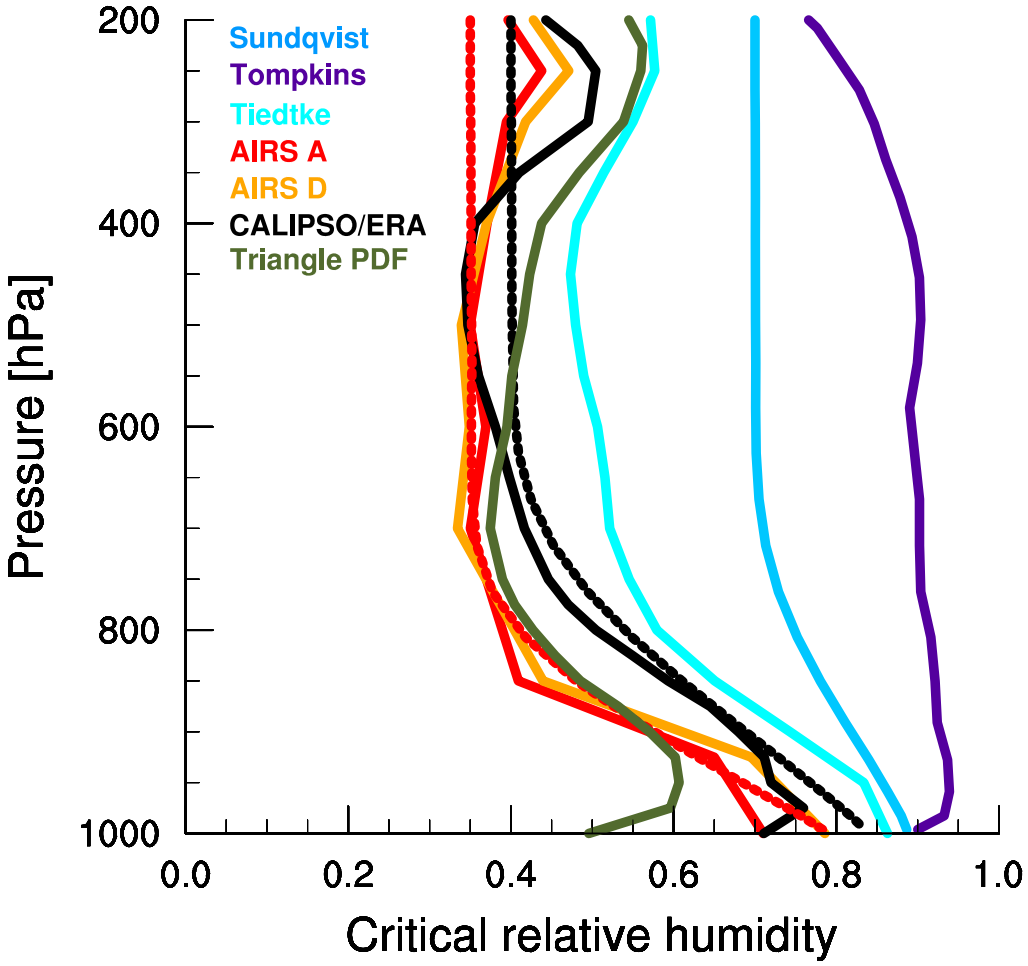

Figure 3: Global-mean profiles of the critical relative humidity from the combined CALIPSO/ERA-Interim data (black), the day- and nighttime data for AIRS (red and orange, respectively), and diagnosed from different GCM parameterisations, namely the Sundqvist et al. (1989, light blue), Tompkins (2002, purple), and Tiedtke (1993, turquoise) parameterisations. The dashed lines are fits of the Sundqvist et al. (1989) parameterisation to CALIPSO/ERA (black) and AIRS (red) data. The olive green line shows the profile derived from CALIPSO/ERA but in a formulation derived assuming a triangular PDF (Smith, 1990).

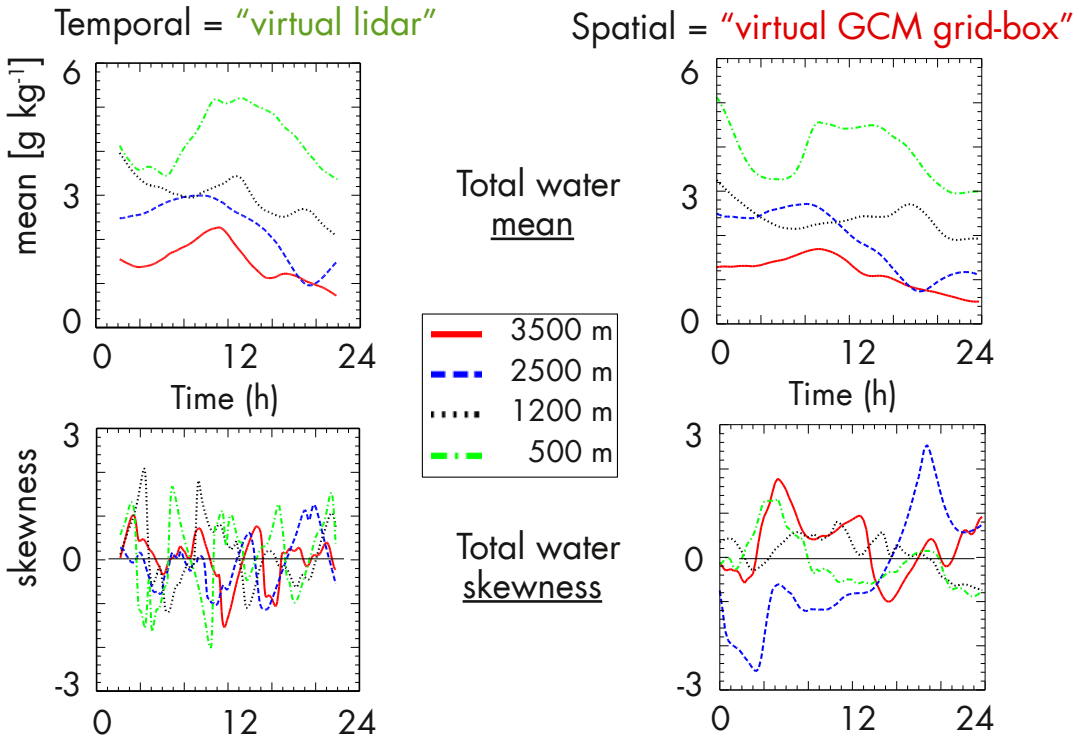

Figure 4: Comparison of temporal and spatial variability in a "virtual relality" framework. Left column: PDF sampled from temporal variability at 15 min. resolution in a time window of 2.8 h corresponding to about 100 km for a wind speed of 10 m s^{-2}. Right column: PDF sampled from horizontal spatial variability at 2.8x2.8 km^2 resolution over a domain of 110x190 km^2 around the "lidar" column. Top row: Mean values. Bottom row: Skewness. The results are shown for four levels at 500 m, 1200 m, 2500 m and 3000 m height above ground.

and thus follows a slightly different profile.

4 Using supersite data for evaluation?

At so-called "supersites", several sounding instruments are available at one single site, sometimes including differential-absorption lidars (DIAL) and/or Raman lidars, allowing to retrieve specific humidity, as well as cloud radars in combination with microwave sounders, allowing to retrieve cloud liquid- and ice water contents. The combination yields at very good vertical and temporal resolution the total water specific humidity. The PDF can be inferred for any time window. In turn, the PDFs used in GCM cloud schemes refer to the horizontal spatial variability. If one can assume ergodicity, then from the wind velocity one can translate temporal into spatial variability. The extent to which this is fulfilled can be tested in the framework of a "virtual reality", i.e., by analysing high-resolution model data. In a one-day simulation with the Consortium for Small-Scale Modelling model (COSMO, Baldauf et al., 2011) for Central Europe we select one COSMO grid column (horizontal resolution 2.8x2.8 km^2) around the Hamburg grid-point where orography and land surface cover are rather homogeneous. For this column, the temporal evolution of the total water specific humidity is analysed. At the same time, the spatial variability in an area of 110x190 km^2 corresponding to a T63 gridbox around this column is analysed.

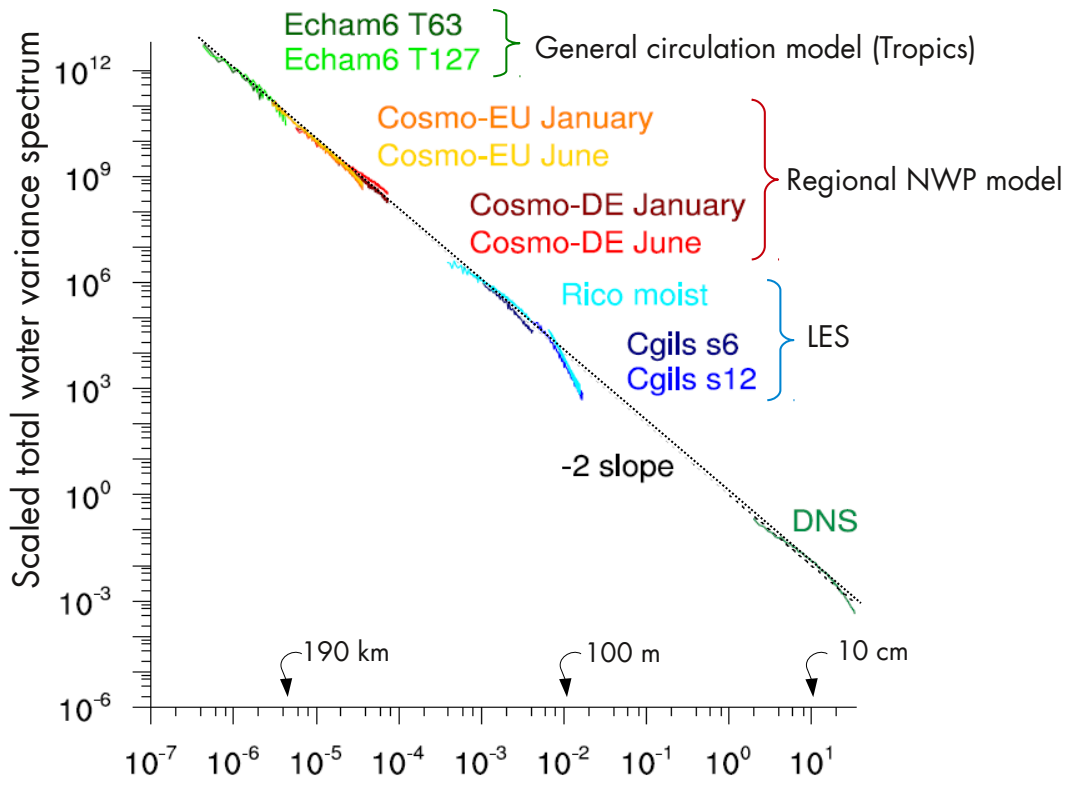

Figure 5: Power spectrum of the total water variance. For each model, the spectrum is re-scaled so all models lie on a common line. The largest and lowest parts of the spectrum for each model, presumably influenced by numerical issues, are omitted. Results from a tropical belt (between 30°S and 30°N) for the general circulation model ECHAM6 (Stevens et al., 2013) are shown at the T63 (approx. 190 km) and T127 (approx. 100 km) resolutions in dark and light green, respectively; results from the regional numerical weather prediction (NWP) model COSMO (Baldauf et al., 2011) for a European domain (7 km resolution) and a German domain (2.8 km), large eddy simulations (LES, Stevens and Seifert, 2008) for different cases at 100 m (s6 case, 96x96 grid-points in the domain) and 25 m (s12 and RICO cases for a domain of 128x128 and 1024x1024 grid points, respectively), respectively, and direct numerical simulations (DNS) at 1024 grid-points in each direction for a 3 m domain (about 3 mm resolution; Mellado, 2010).

We find that the mean values of the total water specific humidity, and their temporal and vertical variability analysed in both ways correspond well (Fig. 4). However, there is little resemblance in either variance or skewness of the q_t PDF from the spatial and temporal ways to diagnose the PDF (Grützun et al., 2013).

5 Scaling of total water variance

Schemann et al. (2013) analyse the power spectra of the total water specific humidity in results from ten different simulations of cloudy situations from models over various domains and at resolutions ranging from 30 mm for direct numerical simualations to 190 km for a general circulation model (Fig. 5). A two-dimensional Fourier analysis of the total water specific humidity was performed for the limited domains (in case of the GCM, only a tropical belt was used in which also in the longitudinal direction grid spacing is appoximately constant). For each of the domains, an intermediate range of scales was

used, since for the upper and lower ends of the analysed wavenumber ranges a deviation from the scaling was found, which might be caused by numerical issues (Schemann et al., 2013). Model levels in which liquid-water clouds occur were selected. For each of the models, a scaling following a power law with an exponent of about -2 was found. The range of exponents was between -4.5±0.5 and -3.9±0.4 for the LES RICO (large wavenumbers) and s12 cases, respectively, and -1.7±0.3 for both the LES RICO (low wavenumbers) and COSMO-DE (June case) simulations, where the uncertainties given are the standard deviations for variability among all timesteps and levels analysed. For all other model simulations, mean exponents between -1.9 and -2.1 were found. Assuming this scaling is correct, the parameterised and extrapolated subgrid-scale variance in the GCM can be evaluated. It was found that for the T63 GCM simulation applying the Tompkins (2002) scheme, a mean subgrid-scale variance of 0.16 g^2 kg^{-2} is expected, while the parameterisation only yields 0.077 g^2 kg^{-2} (Schemann et al., 2013). A revision of the scheme taking this finding into account is planned for the future.

6 Conclusions

Four different approaches to evaluate subgrid-scale variability of total water specific humidity in general ciruclation models, necessary for cloud parameterisations, were presented. The PDF of the vertical integral of q_t, available from satellite spectroradiometers with high spatial resolution, allows for an evaluation of the column-integral results, thus focusing on the boundary layer. A general lack of variance in the Tompkins (2002) scheme as implemented in the ECHAM5 GCM has been found, as well as the need to introduce negative skewness in the boundary layer due to convective downdrafts.
The critical relative humidity is a simple metric available from different observational data sources, and useful to evaluate the subgrid-scale variability at the basis of different cloud parameterisations in a consistent setting. It was found that the Tompkins (2002) and also the original Sundqvist et al. (1989) schemes parameterise too little variance, while the Tiedtke (1993) scheme in the ECMWF model performs better, albeit still underestimates variability. This method relies on the assumption of saturation within clouds, questionable for ice clouds. It is also sensitive to the assumption on the form of the underlying PDF.
We show from an analysis of high-resolved model data that a combination of observations from supersites, of good accuracy and high temporal and vertical resolution, unfortunately is not straightforward to use for the evaluation of higher moments of the total-water PDF.
From a hierarchy of models, we show that total-water variance scales according to a power law with an exponent of about -2. From this, subgrid-scale variance can be estimated, and this information is useful to revise cloud parameterisations.

Acknowledgements

This work was funded by the German Research Foundation (Deutsche Forschungsgemeinschaft, DFG) in an “Emmy Noether” grant, by the “Climate System Analysis and Prediction” (CLISAP) exellency cluster of the University of Hamburg, and by the German Weather Service (Deutscher Wetterdienst, DWD) in an extramural research project. Computing time was provided by the German Climate Computing Centre (Deutsches Klimarechenzentrum, DKRZ). MODIS data are from NASA’s Earth Science Enterprise, produced by the MODIS Science team, and obtained from the Goddard Distributed Active Archive (DAAC). AIRS data were obtained through the Goddard Earth Sciences Data and Information Services Center (online at http://daac.gsfc.nasa.gov). ERA-Interim data used in in this study have been obtained from the ECMWF data server (http://www.ecmwf.int/products/data). GOCCP data were used as provided by the Laboratoire de Météorologie Dynamique/IPSL/CNRS (http://climserv.ipsl.polytechnique.fr).

References

Baldauf, M., A. Seifert, J. Förstner, D. Majewski, M. Raschendorfer, and T. Reinhardt (2011). Operational convective-scale numerical weather prediction with the COSMO model. *Mon. Wea. Rev.* (139), 3887–3905.

Chepfer, H., S. Bony, D. Winker, G. Cesana, J.-L. Dufresne, P. Minnis, C. J. Stubenrauch, and S. Zeng (2010). The GCM Oriented Calipso Cloud Product (CALIPSO-GOCCP). *J. Geophys. Res. 115*, D00H16.

Grützun, V., J. Quaas, F. Ament and C. Morcrette (2013). Evaluating statistical cloud schemes - what can we gain from ground-based remote sensing? *J. Geophys. Res. In press*.

Lohmann, U. and E. Roeckner (1996). Design and performance of a new cloud microphysics scheme developed for the ECHAM general circulation model. *Clim. Dyn. 12*, 557–572.

Mellado, J. P. (2010). The evaporatively driven cloudtop mixing layer. *J. Fluid Mech. 660*, 536.

Platnick, S., M. D. King, S. A. Ackerman, W. P. Menzel, B. A. Baum, C. Riedl, R. A. F. . T. M. cloud products: Algorithms, examples from Terra. IEEE Transactions on Ge oscience, and .-. Remote Sensing, Aqua Special Issue(41) (2003). The MODIS cloud products: Algorithms and examples from Terra. *IEEE Transactions Geosci. Remote Sens. 41*, 459–473.

Quaas, J. (2012). Evaluating the "critical relative humidity" as a measure of subgrid-scale variability of humidity in general circulation model cloud cover parameterisations using satellite data. *J. Geophys. Res. 117*, D09208.

Räisänen, P., H. W. Barker, M. F. Khairoutdinov, J. Li, and D. A. Randall (2004). Stochastic generation of subgrid-scale cloudy columns for large-scale models. *Q. J. R. Meteorol. Soc. 130*, 2047–2067.

Roeckner, E., G. Bäuml, L. Bonaventura, R. Brokopf, M. Esch, M. Giorgetta, S. Hagemann, I. Kirchner, L. Kornblueh, E. Manzini, A. Rhodin, U. Schlese, U. Schulzweida, and A. Tompkins (2003). The atmospheric general circulation model ECHAM5: Part I: Model description. In *Report 349*, pp. 127. Max Planck Institute for Meteorology.

Schemann, V., B. Stevens, V. Grützun, and J. Quaas (2013). Scale dependency of total-water variance, and its implication for cloud parameteriztion. *J. Atmos. Sci. in press*.

Simmons, A., S. Uppala, D. Dee, and S. Kobayashi (2006). ERA-Interim: New ECMWF reanalysis products from 1989 onwards. *ECMWF Newsletter 110*, 25 – 35.

Smith, R. N. (1990). A scheme for predicting layer clouds and their water content in a general circulation model. *Q. J. R. Meteorol. Soc. 116*, 435460.

Stevens, B., M. A. Giorgetta, E. Roeckner, T. Mauritsen, T. Crueger, H. Schmidt, E. Manzini, M. Esch, S. Rast, S. Kinne, L. Kornblueh, and R. Pincus (2013). The atmospheric component of the MPI-M Earth System Model: ECHAM6. *J. Adv. Model. Earth Syst.* , doi:10.1002/jame.20015.

Stevens, B. and A. Seifert (2008). On the sensitivity of simulations of shallow cumulus convection to their microphysical representation. *J. Meteorol. Soc. Japan 86A*, 143–162.

Sundqvist, H., E. Berge, and J. E. Kristjánsson (1989). Condensation and cloud parameterization studies with a mesoscale numerical weather prediction model. *Mon. Wea. Rev. 117*, 1641–1657.

Susskind, J., C. D. Barnet, and J. M. Blaisdell (2003). Retrieval of atmospheric and surface parameters from AIRS/AMSU/HSB data in the presence of clouds. *Geosci. Rem. Sens. IEEE Transact. 41*, 390 – 409.

Tiedtke, M. (1993). Representation of clouds in large scale models. *Mon. Weather Rev. 121*, 30403061.

Tompkins, A. (2002). A prognostic parameterization for the subgrid-scale variability of water vapor and clouds in large-scale model and its use to diagnose cloud cover. *J. Atmos. Sci. 59*, 1917–1942.

Weber, T., J. Quaas, and P. Räisänen (2011). Evaluation of the subgrid-scale variability scheme for water vapor and cloud condensate in the echam5 model using satellite data. *Quart. J. Royal Meteorol. Soc. 137*, 2079–2091.